

# A Pattern Language for Machine Learning Tasks

Benjamin Rodatz<sup>\*‡†</sup>      Ian Fan<sup>\*†</sup>      Tuomas Laakkonen<sup>†</sup>  
Neil John Ortega<sup>†</sup>      Thomas Hoffman<sup>†</sup>      Vincent Wang-Maścianica<sup>\*†‡#</sup>

<sup>†</sup>Compositional Intelligence, Quantinuum  
17 Beaumont St., Oxford OX1 2NA, UK  
first.last@quantinuum.com

<sup>‡</sup>Department of Computer Science, University of Oxford  
7 Parks Rd, Oxford OX1 3QG, UK

## Abstract

Idealised as universal approximators, learners such as neural networks can be viewed as “variable functions” that may become one of a range of concrete functions after training. In the same way that equations constrain the possible values of variables in algebra, we may view objective functions as constraints on the behaviour of learners. We extract the equivalences perfectly optimised objective functions impose, calling them “tasks”. For these tasks, we develop a formal graphical language that allows us to: (1) separate the core tasks of a behaviour from its implementation details; (2) reason about and design behaviours model-agnostically; and (3) simply describe and unify approaches in machine learning across domains.

As proof-of-concept, we design a novel task that enables converting classifiers into generative models we call “manipulators”, which we implement by directly translating task specifications into code. The resulting models exhibit capabilities such as style transfer and interpretable latent-space editing, without the need for custom architectures, adversarial training or random sampling. We formally relate the behaviour of manipulators to GANs, and empirically demonstrate their competitive performance with VAEs. We report on experiments across vision and language domains aiming to characterise manipulators as approximate Bayesian inversions of discriminative classifiers.

## 1 Introduction

The primary instrument for controlling the training of machine learning (ML) models is the objective function, which we can view as a map from possible parameters of the model to a real number we call the loss. Designing a good objective function incorporates many empirical choices, such as choice of architecture, measure of statistical divergence, and training data (Ciampiconi et al. 2023; Richardson 2022; Terven et al. 2023), that are often chosen by heuristics, and rationalised post hoc. Though many of these choices are required to make training tractable, they are not relevant to understanding the final behaviour of the trained model. Instead, we propose that an essential to understanding model behaviour is the specification of the behavioural equivalences achieved if the objective function is perfectly optimised.

---

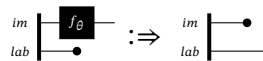
<sup>\*</sup>Equal contribution

<sup>#</sup>Corresponding author (vincent.wang@quantinuum.com)

An objective function can be broken into three parts. Let  $\Theta$  be the parameter-space of a model  $f$ . Then a generic supervised classification task — for example, labelling images — amounts to minimising (for  $\theta \in \Theta$ ) the following objective function:

$$\mathbb{E}_{(im,lab) \sim \mathcal{X}} [\mathbf{D}(f_{\theta}(im), lab)]$$

Firstly, we take the **expected value over some data distribution** of paired images  $im$  with their labels  $lab$ . Secondly, we choose a **measure of statistical divergence  $\mathbf{D}$** , such as cross-entropy or log-likelihood. Finally, we have the **two sides that, under perfect conditions, should be equal**: the output of the classifier  $f_{\theta}$  given an image  $im$  and the matching label  $lab$ . In this work, we focus on the final aspect: the two things we want to be equal. We call this equational constraint a task to distinguish it from the objective function. Further, we abstract away implementation details, such as architecture and training, by idealising models to be universal function approximators that can, in principle, perfectly optimise objective functions. Thus each task can be viewed purely as an equational constraint on the behaviour of the learners, comparable to equational constraints on the possible values of variables in algebra. We can compactly notate such tasks as directed equations between string diagrams:



The potential of this mathematics is the ability to systematically compose objective functions that yield desired behaviours in ML models by composing task specifications like the one above, ultimately seeking formal guarantees. This style of engineering is already common practice in many fields of ML, and all we seek to do here is place these practices on more rigorous footing. Task 2.8 and Propositions 2.13, 3.3, and 3.5 illustrate the kinds of formal reasoning our language enables.

As a practical proof-of-concept, we design and implement a task we call **manipulation** (Section 3) inspired by Bidirectional Transformations (BX) (Abou-Saleh et al. 2018), which formalises the problem of viewing and editing a targeted attribute of data while “leaving other aspects the same”: for instance, changing whether a person is smiling in an image (Figure 4) while preserving other features. Directly translating our mathematical task specifications to objective functions obtains a family of architecture-agnostic (Table 1) style-transference models (Section 3.3) that perform comparably to VAEs as generative classifiers (Figure 5) without the need for randomness, adversarial training, or modality- and architecture-specific interventions (Section 3.1, Figure 2, Figure 3), simultaneously permitting outputs to be conditioned on a target class and a reference input for style (Figures 1, 4, 5). Furthermore, we demonstrate its capabilities as a practical interpretability tool that allows us to probe and reshape latent space representations (Section 3.2, Figure 4).

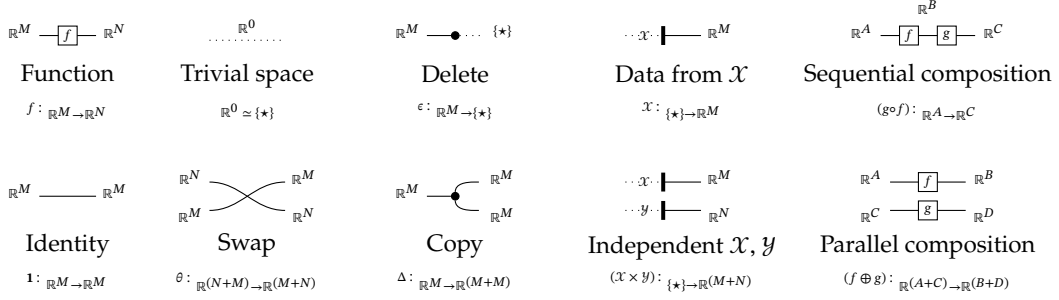
## 2 Tasks and patterns

### 2.1 Mathematical preliminaries

We proceed using string diagrams, which formally represent composite processes in an intuitive diagrammatic syntax, and are employed in a variety of fields<sup>1</sup>. String diagrams are built using

<sup>1</sup>Examples include linear and affine algebra (Bonchi, Piedeleu, et al. 2019; Bonchi, Sobocinski, and Zanasi 2017; Paweł Sobociński 2015), first order logic (Haydon and Paweł Sobociński 2020), causal models (Jacobs, Kissinger, and Zanasi 2019; Lorenz and Tull 2023), signal flow graphs (Bonchi, Paweł Sobociński, and Zanasi 2014), electrical circuits (Boisseau and Paweł Sobociński 2022), game theory (Hedges 2015), petri nets (Baez and Master 2020), probability theory (Fritz, Gonda, and Perrone 2021), formal linguistics (Coecke, Sadrzadeh, and Clark 2010; Wang-Mascianica, J. Liu, and Coecke 2023), quantum theory (Coecke and Duncan 2011; Coecke and Kissinger 2017; Poór et al. 2023), and aspects of machine learning such as backpropagation (Cruftwell et al. 2022).

sequential and parallel composition from the following generators (category-theoretic details in Appendix A):



An attractive characteristic of string diagrams is that visually intuitive equivalences between information flows are guaranteed to correspond to symbolic derivations of behavioural equivalence: tedious algebraic proofs of equality between sequentially- and parallel-composite processes are suppressed and absorbed by (processive) isotopies of diagrams. In the diagrammatic syntax it is conventional to notate such isomorphisms as plain equalities. Interested readers are referred to (Selinger 2011) for the mathematical foundations.

$$\begin{aligned}
& (\mathbf{1} \oplus \theta) \circ (\Delta \oplus g) \circ (f \oplus \mathbf{1}) \\
& \simeq (\mathbf{1} \oplus \theta) \circ (\mathbf{1} \oplus \mathbf{1} \oplus g) \circ (\Delta \oplus \mathbf{1}) \circ (f \oplus \mathbf{1}) && \text{[Identity, interchange]} \\
& \simeq (\mathbf{1} \oplus g \oplus \mathbf{1}) \circ (\mathbf{1} \oplus \theta) \circ (\Delta \oplus \mathbf{1}) \circ (f \oplus \mathbf{1}) && \text{[Braid naturality]} \\
& \simeq (\mathbf{1} \oplus g \oplus \mathbf{1}) \circ (\mathbf{1} \oplus \theta) \circ (f \oplus f \oplus \mathbf{1}) \circ (\Delta \oplus \mathbf{1}) && \text{[Copy naturality]} \\
& \simeq (\mathbf{1} \oplus g \oplus \mathbf{1}) \circ (f \oplus \mathbf{1} \oplus f) \circ (\mathbf{1} \oplus \theta) \circ (\Delta \oplus \mathbf{1}) && \text{[Braid naturality]}
\end{aligned}
\quad \Leftrightarrow \quad
\begin{array}{c}
\text{Diagram 1: } \mathbb{R}^M \text{ wire } \xrightarrow{f} \mathbb{R}^N \text{ wire} \\
\text{Diagram 2: } \mathbb{R}^M \text{ wire } \xrightarrow{f} \mathbb{R}^N \text{ wire} \\
\text{Diagram 3: } \mathbb{R}^M \text{ wire } \xrightarrow{f} \mathbb{R}^N \text{ wire}
\end{array}
=
\begin{array}{c}
\text{Diagram 4: } \mathbb{R}^M \text{ wire } \xrightarrow{f} \mathbb{R}^N \text{ wire} \\
\text{Diagram 5: } \mathbb{R}^M \text{ wire } \xrightarrow{f} \mathbb{R}^N \text{ wire} \\
\text{Diagram 6: } \mathbb{R}^M \text{ wire } \xrightarrow{f} \mathbb{R}^N \text{ wire}
\end{array}$$

## 2.2 Learners as universal approximators

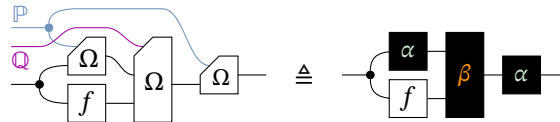
As we are concerned with behaviour, not implementation details, we idealise all neural networks as perfect universal approximators, which we may formulate string-diagrammatically (Pavlovic 2013, 2023). In essence, we are assuming that architectures are sufficiently expressive to optimise whatever tasks we give them; in practice, the conditions under which architectures become universal approximators can be mild (Hornik, Stinchcombe, and White 1989), and the idealisation is increasingly true-in-practice in the contemporary context of increasing data and compute.

**Definition 2.1** (Learner). Let  $X, Y$  denote input and output types. A process  $\Omega: \mathbb{P} \oplus X \rightarrow Y$  with parameters in  $\text{para}(\Omega) = \mathbb{P} = \mathbb{R}^n$  (for sufficiently large  $n$ ) is a *universal approximator* or *learner* when<sup>2</sup>:

$$\forall f_{X \rightarrow Y} \exists f_{\in \mathbb{P}} : \quad X \xrightarrow{f} Y = \begin{array}{c} \mathbb{P} \\ \triangleleft \\ X \xrightarrow{\Omega} Y \end{array}$$

The parameter space could represent e.g. the phase space of weights and biases of a neural network.

**Example 2.2.** By visual convention, we use colours to indicate different data types of wires. We depict processes with no free parameters as white boxes, and learners as black-boxes with variable labels to indicate distinct or shared parameters. The following composite process has one function  $f$  with no learnable parameters, and three neural nets: the two labelled  $\alpha$  share a parameter in the space  $\mathbb{P}$ , and the one labelled  $\beta$  takes a parameter in  $\mathbb{Q}$ . In this paper, we favour the shorthand on the right.



<sup>2</sup>We adapt the shape of the universal approximators to clearly indicate the parameters.

## 2.3 Tasks

We assume the following contextual data, omitted if there is no confusion. Let  $X, Y$  denote datatypes;  $\Sigma$  a set of processes  $f$ , each of which has (possibly empty) learnable parameter datatypes  $\mathbb{P}_f$ .

**Definition 2.3** (Tasks). An *atomic task*  $\varphi$  is a tuple  $(f, g, \mathcal{X}, \mathbb{P})$ , where  $f, g : X \rightarrow Y$  are composite processes of  $\Sigma$ ,  $\mathcal{X}$  is a distribution over  $X$ , and  $\mathbb{P} \subseteq \mathbb{P}_f \oplus \mathbb{P}_g$  is a space of trainable parameters. We indicate the *system*  $f$  and *specification*  $g$  as  $\text{sys}_\varphi$  and  $\text{spec}_\varphi$ , and similarly the *domain*  $X$  and *codomain*  $Y$  as  $\text{dom}(\varphi)$  and  $\text{cod}(\varphi)$ . A *compound task*  $\Phi$  (or just *task*) is a non-empty set of tasks.

An atomic task is a process-theoretic equational constraint on learners specifying that  $f$  should behave like  $g$  on all inputs. Translating constraints into objective functions to be minimised allows learners to solve for the equational constraints they occur in, like solving for variables in algebra. The objective function of an atomic task  $\varphi$  of type  $X \rightarrow Y$  equipped with distribution  $\mathcal{X}$  corresponds to a map  $\mathbb{P}_\varphi \rightarrow \mathbb{R}$  that sends  $\pi \mapsto \mathbb{E}_{x \sim \mathcal{X}}[\mathbf{D}(\text{sys}_\varphi(\pi, x), \text{spec}_\varphi(\pi, x))]$  for some choice of statistical divergence  $\mathbf{D}$ . Compound tasks may be learnt by combining atomic objective functions.

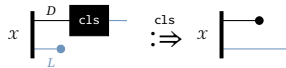
**Definition 2.4** (Objective function). Let  $\Phi = \{(f_i, g_i, \mathcal{X}_i, \mathbb{P}_i)\}_{i \in N}$  be a compound task with  $N$  atomic tasks. Let  $l \in \Sigma$  be a learner of  $\Phi$ . An *objective function* for  $l$  is a tuple  $(\Phi_l, \mathcal{D}, \alpha)$  where  $\Phi_l = \{(f_i, g_i, \mathcal{X}_i, \mathbb{P}_i) \mid \text{para}(l) \subseteq \mathbb{P}_i\}$  is the set of all tasks on which  $l$  is optimised,  $\mathcal{D}$  is a set of *statistical divergences*  $\mathbf{D}_{(\varphi \in \Phi_l)} : \text{cod}(\varphi) \times \text{cod}(\varphi) \rightarrow \mathbb{R}^{\geq 0}$ , and the *compound function*  $\alpha$  is a function  $(\mathbb{R}^{\geq 0})^{\times |\Phi_l|} \rightarrow \mathbb{R}^{\geq 0}$  that is non-decreasing in each argument.

The objective function for  $l$  then corresponds to the output of the compound function  $\alpha$  given the losses of the atomic tasks. A common compound function is a weighted sum.

## 2.4 Patterns

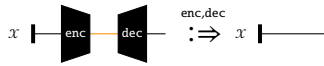
Some tasks are well understood, efficiently reusable, and easily modifiable. These qualities are usually not mathematically definable, but agreed upon by convention. Such intuitive tasks can be viewed as *patterns* – borrowing a term from software engineering (Beck and Cunningham 1987)<sup>3</sup>. We suggest some examples of patterns, and how to use them as an accessible basis to informally analyse existing approaches to ML problems. By convention, we distinguish tasks (e.g. autoencoding) from the models and objective functions (e.g. autoencoders and reconstruction loss) that perform the tasks.

**Pattern 2.5** (classification).



Given a data-label pair  $(d, l)$  drawn from  $\mathcal{X}$  with labels  $l \in L$ , a *classifier*  $\text{cls} : D \rightarrow L$  is a function that solves the classification task, in which it seeks to reconstruct the label from the data. This can be done by minimising the corresponding objective function  $\mathbb{E}_{(d,l) \sim \mathcal{X}}[\mathbf{D}(\text{cls}(d), l)]$  for some measure of statistical divergence  $\mathbf{D}$  on the label space.

**Pattern 2.6** (autoencoding).



Given a data distribution  $\mathcal{X}$  over  $X$  and some latent space  $LAT$ , an *autoencoder* consists of an *encoder*  $\text{enc} : X \rightarrow LAT$  and a *decoder*  $\text{dec} : LAT \rightarrow X$  which cooperate to reconstruct the identity over the observed distribution.

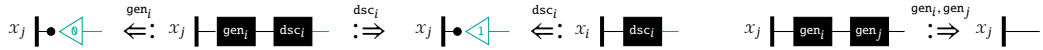
<sup>3</sup>And before that, architecture and urban design (Alexander, Ishikawa, and Silverstein 1977).

**Pattern 2.7 (GAN).** Given a data distribution  $\mathcal{X}$  over  $X$  and noise distribution  $\mathcal{N}$  over  $N$ , a *generative adversarial network* (GAN) consists of a *generator*  $\text{gen} : N \rightarrow X$  and a *discriminator*  $\text{dsc} : X \rightarrow [0, 1]$ . The prosaic explanation that the discriminator seeks to distinguish real data from fake data while the generator aims to fool the discriminator translates directly into a task description.

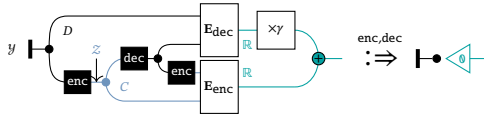


By using patterns as intuitive building blocks, we can analyse the intended functions of more complicated tasks by viewing them as composites of simple patterns.

**Task 2.8 (CycleGAN).** A CycleGAN is two GANs on different distributions, whose generators are mutually autoencoders by the *cycle consistency loss* (Zhu et al. 2017). This suggests that the generators encode the distributions into each other in a reversible manner, and indeed this kind of style transfer between distributions is what a CycleGAN does in practice.



**Pattern 2.9 (energy minimisation).**



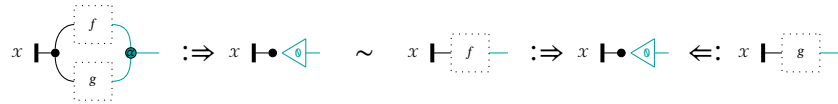
We can also upgrade informal intuitions into formal derivations. For example, on the account of Ranzato et al. (Ranzato et al. 2007), a broad class of unsupervised learning techniques, including PCA and  $k$ -means, are specialisations of the *energy minimisation* architecture, which consists of: three types of systems:  $D(\text{ata})$ ,  $C(\text{ode})$ , and  $\mathbb{R}^{\geq 0}$ ; two learnable processes: an encoder  $\text{enc} : D \rightarrow C$  and a decoder  $\text{dec} : C \rightarrow D$ ; two user-supplied *energy functions*:

$\mathbf{E}_{\text{enc}} : C \times C \rightarrow \mathbb{R}^{\geq 0}$  and  $\mathbf{E}_{\text{dec}} : D \times D \rightarrow \mathbb{R}^{\geq 0}$ ; and a user-supplied constant  $\gamma \in \mathbb{R}^{\geq 0}$ . Provided a distribution of inputs  $\mathcal{Y}$  of  $D$ , and a distribution  $\mathcal{Z}$  of  $C$  the system seeks to minimise  $\mathbb{E}_{y \sim \mathcal{Y}, z \sim \mathcal{Z}} [\gamma \mathbf{E}_{\text{enc}}(\text{enc}(y), z) + \mathbf{E}_{\text{dec}}(y, d(z))]$ . Such an architecture is called *code-extracting* when  $\mathcal{Z} \triangleq \text{enc}(\mathcal{Y})$ , which is what we depict in the pattern. We can formally elaborate on the relationship between energy-minimisation and autoencoders.

**Definition 2.10 (Refinement and equivalence of tasks).** Task  $\Phi$  *refines* task  $\Psi$  if, by treating the atomic tasks as equations, the processes of  $\Phi$  may be composed to satisfy the equations of  $\Psi$ .  $\Phi$  and  $\Psi$  are *equivalent* if they refine one another, which we denote  $\Phi \sim \Psi$ .

Refinement asks if perfectly solving  $\Phi$  yields solutions for  $\Psi$ . This is a useful relationship to compare the relative power or behaviour of the concrete implementation of tasks (though theory may not always translate to practice). We illustrate this style of reasoning below.

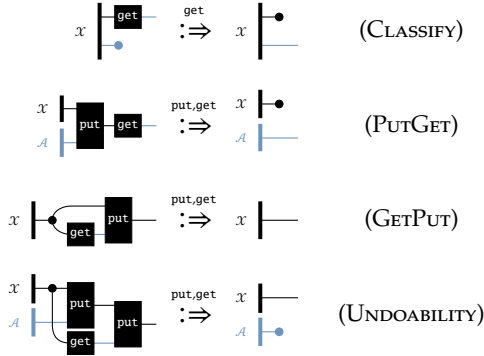
**Lemma 2.11.** For any positive linear combination  $\alpha : \mathbb{R}^{\geq 0} \times \mathbb{R}^{\geq 0} \rightarrow \mathbb{R}^{\geq 0}$ :



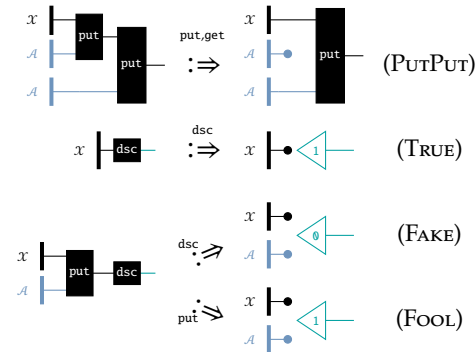
*Proof.* Without loss of generality, let  $\alpha(-, =) = \alpha_1(-) + \alpha_2(=)$ . For the forward refinement, we may assume that for all  $x \in \mathcal{X}$ ,  $\alpha(f(x), g(x)) = \alpha_1(f(x)) + \alpha_2(g(x)) = 0$ . This implies that  $\alpha_1(f(x)) = \alpha_2(g(x)) = 0$ , and since  $\alpha_1, \alpha_2 \in \mathbb{R}^{\geq 0}$ , then  $f(x) = 0 = g(x)$ , which is the desired task. For the backwards refinement, if  $f(x) = 0 = g(x)$  for all  $x \in \mathcal{X}$ , then  $\alpha(f(x), g(x)) = \alpha_1(f(x)) + \alpha_2(g(x)) = 0$ .  $\square$



**Task 3.1 (manipulation).**



**Task 3.2 (strong manipulation add-ons).**



We find in practice that manipulation alone suffices to recover desirable behaviours in simple domains, and in the following sections we report on our empirical investigations relating manipulation to other generative models, concerns in interpretability, and Bayesian inversion.

By convention, just as classifiers classify, we refer to the ensemble of learners put and get as manipulator when they are trained against the tasks above.

**3.1 Manipulating labelled and derived attributes**

We run an initial proof-of-concept of the manipulation task on a simple analytic dataset inspired by Spriteworld (Watters et al. 2019). Each image depicts a single shape with varying properties, and is labelled by two attributes: shape – circle, square or triangle – and colour – red, green or blue. For each attribute, we train a get/put pair according to the manipulation task specification. We find that directly implementing this specification in code is sufficient for training a model that not only classifies the attribute of arbitrary images, but also manipulates each attribute while preserving other properties of the image (Figure 1). Thus, we achieve deterministic (c.f. VAEs (Kingma and Welling 2022)), non-adversarial (c.f. GANs (Goodfellow et al. 2020)), class-conditional generation without hardcoding the labels in latent spaces (c.f. (Shaikh et al. 2022)).

Furthermore, the task can train with even simple choices in implementation details, which reinforces our claim that clear task specification is the crux of understanding model behaviour. This allows us to optimise the training regime without fear of corrupting the integrity of the task itself. For instance, we can add structure to the architecture by nesting patterns. In step (1), we decompose the put into an autoencoder and a learner put' that acts on the latent space. Then, in (2), we decompose put' into a linear addition in latent space, where put'' identifies a single shift vector

Let  $\mathcal{X} : (d, a)$  be a distribution over some data  $d \in D$ , each labelled with an attribute  $a \in A$ . A manipulation consists of a pair of operations ( $\text{get} : D \rightarrow A$ ,  $\text{put} : D \otimes A \rightarrow D$ ) which obey the tasks on the left. Specifically, CLASSIFY asks for get to act as a classifier, and the remaining rules are so-called ‘‘lens laws’’. Optionally, we can add more stringent requirements to obtain strong manipulation with additional behavioural guarantees, at the cost of practical difficulties in training. Concretely, PUTPUT strengthens UNDOABILITY as a memorylessness condition, and we include a GAN pattern that introduces an adversarial discriminator  $\text{dsc} : D \rightarrow [0, 1]$  which guards against failure cases where the put and get collude by taking manipulated data out of distribution. The put performs style-transfer conditioned on a reference datum and target attribute, and we can partially characterise the behavioural properties of put by the following refinement result.

**Proposition 3.3.** Under mild assumptions, an optimal strong manipulator yields optimal generators of a CycleGAN. (proof in Section B.1)

that is dependent only on the value of the input value.



While it is harder for the form of `put` in (2) to perfectly satisfy the atomic tasks of manipulation, such as `GETPUT`, there are several benefits, such as stabler training. Additionally, we can identify vectors in the latent space that correspond to concepts of interest between which we may interpolate to obtain continuous transformations between normally discrete class labels (Figure 1).

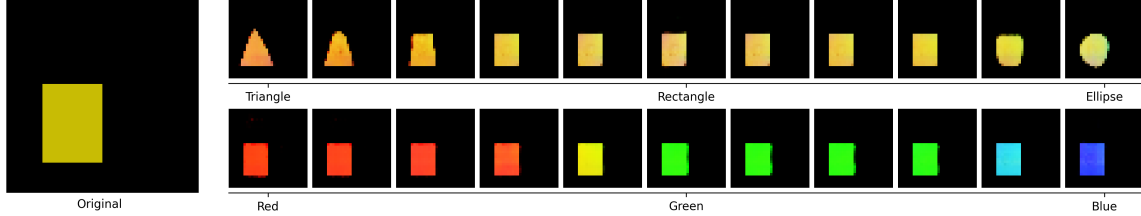


Figure 1: An input Spriteworld image alongside a spectrum of outputs exhibiting the ability of the `put` to not only manipulate a single attribute of the input while preserving its other properties, but interpolate cleanly between the possible values of the attribute. Furthermore, the model is able to generalise to inputs not seen during training, in this case an orange shape (during training, it only sees red, green or blue). (details in Section C.1)

In general, we may be interested in non-explicit attributes that are derived from those labelled in the data. For instance, “eligibility for a loan” may be derived from other explicit attributes of people in a database by an operationally opaque classifier. We call these *derived attributes*. While it is straightforward to handcraft interpretable latent spaces for explicit labels, it can be difficult to do the same for derived attributes, since their range, distribution, and dependencies on other attributes may not be known beforehand. However, since the manipulator is trained end-to-end, it can also be trained for derived attributes. To illustrate this, we define a derived attribute on the Spriteworld data called *blue-circleness*, which broadly measures how similar a shape is to a blue circle (Figure 2).

$$bc = \begin{cases} \min(1, cs + 0.6) & \text{if } shape = circle \\ \min(0.8, \max(0.2, cs)) & \text{if } shape = square \\ \max(0, cs - 0.6) & \text{if } shape = triangle \end{cases}$$

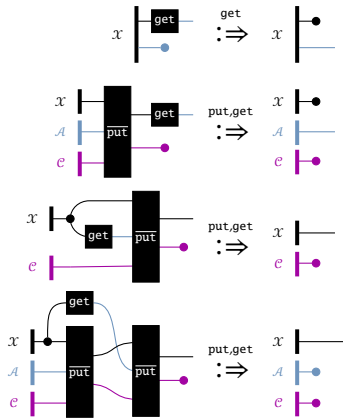
Figure 2: We define *blue-circleness* ( $bc$ ) as a function of explicit attributes *shape* and *colour*; we assign a continuous colour score  $cs \in [0, 1]$  based on the hue, where red = 0 and blue = 1. The primary obstacle for `put` is differing entropy in the classes. The class 0 has higher entropy than 0.4 because there are more shapes that have  $bc$ -value 0. So manipulating a shape with  $bc$ -value 0 to 0.4 must lose information, which makes `UNDOABILITY` impossible to satisfy without additional assumptions.

On the account of (Chu, Zhmoginov, and Sandler 2017), unsupervised image translation can be viewed as learning bijections in the attribute classes. One challenge in manipulating derived attributes is unequal entropy (illustrated in Figure 2). For CycleGANs, unequal entropy can cause them to hide data imperceptibly, making such models particularly vulnerable to adversarial attacks, for which various solutions have been proposed<sup>4</sup>.

<sup>4</sup>Examples in the image setting include: masks (Wu et al. 2024), blurring (Fu et al. 2019) and compression (Dziugaite, Ghahramani, and Roy 2016).



**Task 3.4 (complement manipulation).**



We can overcome this challenge without modifying images by once again borrowing from bidirectional transformations: inspired by the complement of symmetric lenses (Hofmann, Pierce, and Wagner 2011), we introduce a complement  $C$  to put, changing its type to  $S \times L \times C \rightarrow S \times C$ .

Let  $x : (d, a)$  be a distribution over some data  $d \in D$ , each labelled with an attribute  $a \in A$ . A complement manipulator consists of a pair ( $\text{get} : D \rightarrow A, \overline{\text{put}} : D \otimes A \otimes C \rightarrow D \otimes C$ ) fulfilling the rules on the left. The idea of the complement is that it provides the manipulator with a scratchpad  $C$  to keep track of additional data. As none of the tasks check the output of the complement, the manipulator can use it freely.

As shown in Figure 3, the concept manipulator can successfully edit attributes with unequal entropy.

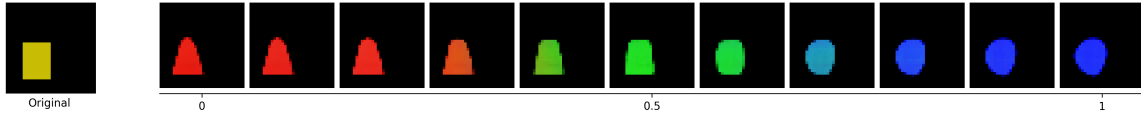


Figure 3: Complement manipulators (Task 3.4) can manipulate derived attributes such as *blue-circleness*, by using the complement as a scratchpad to record a correspondence between data points (details in Section C.1).

### 3.2 Non-analytic data and interpretable latent spaces

We also train manipulation on real data, such as the *Large-scale CelebFaces Attributes* dataset (Z. Liu et al. 2015), where we target the non-trivial attribute of whether a person is smiling. Again, by simply implementing the task specification in code with basic implementation choices, we are able to train a model that is able to both classify and manipulate the degree to which a person in the image is smiling (Figure 4, left). Furthermore, we demonstrate the additional capability of this framework to control latent space representations. By specifying the manipulator to be linear, i.e. the change in latent space is defined to be a vector that is solely dependent on the target attribute and not the image, we can train the autoencoder in tandem with the manipulator to encourage it to separate the embeddings of smiling and non-smiling images in a linear direction (Figure 4, right).

### 3.3 Manipulators as generative classifiers

Borrowing terminology from (Ng and Jordan 2001), classifiers are *discriminative* if they seek to learn the conditional distribution  $p(a|d)$  of attributes given data (as in the classification pattern), and otherwise they are *generative* if they seek to learn the joint distribution  $p(d, a)$  (as, for example, a VAE). The tradeoffs between the two types are well studied, e.g. performance-wise, generative models may converge faster with limited data, but discriminative models often achieve lower asymptotic error, and it is well known that learning generative models is harder (Vapnik 1998). In this section we provide evidence manipulators are generative classifiers in the terminology above in a strong sense, as the put appears to approximate the Bayesian inverse of any given discriminative classifier as the get; informally, this would make the put “the best generative counterpart” of a discriminative classifier. We first identify theoretical conditions under which manipulators can achieve Bayesian inversion in this way.

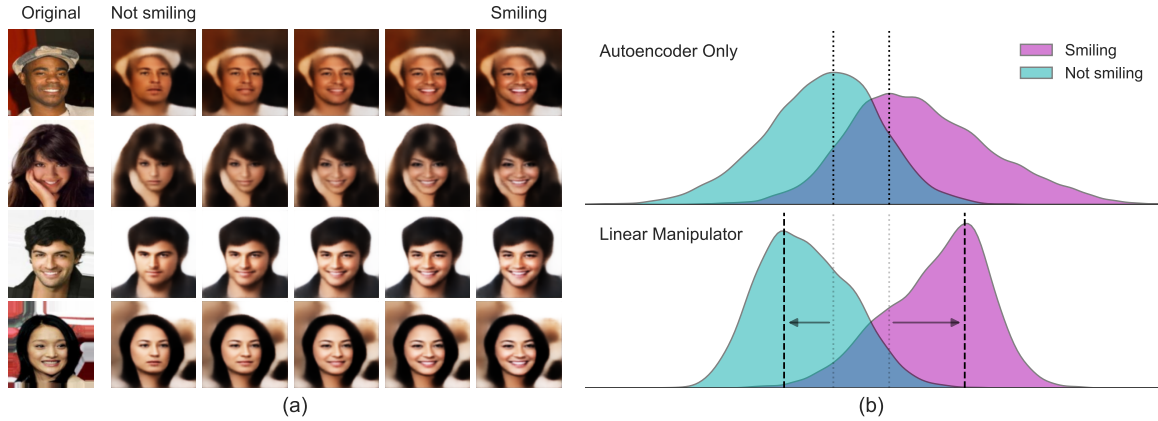


Figure 4: *Left*: Outputs of a linear manipulator trained on face image data paired with a binary “smile”/“no-smile” label. *Right*: A comparison of the spread of the latent embeddings of images from the validation set when pre-training an autoencoder and then training a (linear) classifier on the latent space (top), vs. when trained with a linear manipulator (bottom). The graphs show the density of embeddings along the direction of the classifiers’ weight vectors, normalised so that each combined data spread is centred and has unit variance (details in Section C.2).

**Proposition 3.5** (strong manipulation as Bayesian inversion). If a discriminative classifier  $\text{cls} : D \rightarrow A$  induces a balanced attribute  $\text{cls}(\mathcal{D})$  over  $A$ , there exists a strong manipulator for which the put induces the Bayesian inversion  $\text{cls}^\dagger : A \rightarrow D$ . (proof in Section B.2)

Outside of the equal entropy assumptions and the guarantees of strong manipulation, we resort to empirical experiments. We first report a result that suggests puts are “informationally identical” to their gets. A priori, we may expect that having puts and gets with different inductive biases (e.g. MLP vs. CNN) could allow synthetic outputs from the put to bootstrap the performance of the get when given access to the same data as a plain classifier. We find that in supervised, unsupervised, and active learning settings for MNIST, there is, at best, no statistically significant difference in the performance of the get compared to a plain classifier for any of our interventions.

Second, as generative classifiers, manipulators appear to approximate the Bayesian inverse of a discriminative classifier  $\text{cls}$ , approximately as well as VAEs do. We tried three ways to train another “informationally identical”  $\text{cls}'$ , provided access to unlabelled data to obtain a distribution of pairs  $(d, \text{cls}(d))$  by: (a) directly training  $\text{cls}$  by classification, (b) training a generative classifier, in our case a VAE, and (c) training manipulation around  $\text{cls}$ -as-get to obtain a put, and then train  $\text{cls}'$  to satisfy the tasks of manipulation except for CLASSIFY. Iterating these processes and observing the rate of degradation of successively copied classifiers gives us a qualitative comparison of the difficulty of learning a put (see Figure 5, details in Section C.3).

### 3.4 manipulation in complex modalities

VAEs suffer from posterior collapse (Bond-Taylor et al. 2022) in highly structured domains such as video (Babaeizadeh et al. 2018) and text (Bowman et al. 2016). In this regard, manipulators are similar: our attempts to autoregressively manipulate the sentiment of IMDB reviews often resulted in a form of posterior collapse where put ignored the attribute and behaved as the identity function on text. So instead, we attempted to fine-tune an extant strong solution for sentiment modification by additionally imposing the constraints of manipulation on top of the original objective function. Our findings suggest that additionally imposing the constraints of manipulation on architectures that are already performant does not make a difference (Table 1).

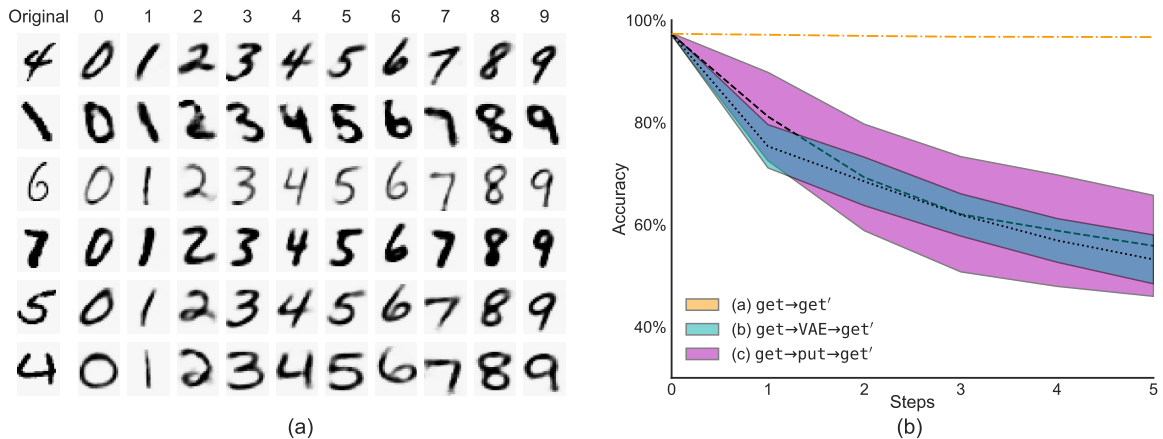


Figure 5: *Left*: outputs of a put trained against an MNIST classifier. We can observe reference-conditioned style-transfer of several graphological aspects, such as stroke weight, slant, and angularity. *Right*: The results of training successive MNIST classifiers using methods (a), (b) and (c) given above. ‘steps’ refers to the number of times this process was repeated. We observe that the degradation of accuracy is approximately the same for both (b) and (c). Both models had roughly the same number of parameters (300K) and were based on the same MLP architecture. We ran 20 repetitions of each method, the shaded regions represent one standard deviation (method (a) had a standard deviation of less than 1%).

MODEL	GLEU	BLEU <sub>SRC</sub>	BLEU <sub>REF</sub>	ACC (FASTTEXT)
B-GST-pretrained	11.869	74.563	52.770	84.6
B-GST-only	11.426	<b>74.876</b>	52.549	<b>85.7</b>
manipulation-only	11.712	74.428	52.646	84.1
B-GST+manipulator	11.338	74.608	<b>52.836</b>	85.1
Human Reference	100.00	58.158	100.00	67.6

Table 1: We pretrained the Blind Generative Style Transformer (**B-GST**) model (Sudhakar, Upadhyay, and Maheswaran 2019) based on the Delete-Retrieve-Generate (Li et al. 2018) framework for sentiment modification until we recovered higher baselines than reported by the authors of the model (GLEU=11.6, BLEU<sub>SRC</sub>=71.0), and we continued training in three different conditions: (1) keeping the original objective, (2) only using objective functions obtained from manipulation, and (3) using both. We report no statistically significant differences in scores, even under continued training. Below we report the results of training conditions (1) and (2) for an additional epoch, and (3) for two epochs (details in Section C.4).

## 4 Discussion

We presented a novel language for representing and reasoning about the behaviour of machine learning models in terms of tasks. We showcased how to relate different models, create new models with desired behaviour, and we explored the potential of this language by proposing and empirically testing a new task we called *manipulation*.

In the experiments presented here, we have aimed for breadth of coverage in tandem with and supporting theoretical development, with a focus on demonstrating the existence of potential avenues by providing proof-of-concept. Accordingly, while none of the products of our experimentation are state-of-the-art with respect to specific applications, the variety and promise of these results serve as a compelling validation of our framework’s utility and potential.

To our knowledge, this is the first practically demonstrated synthesis of insights from BX with ML. This suggests promising future possibilities of our mathematical framework in bridging structural-

symbolic approaches from computer science more broadly with methods that can effectively leverage computation (Sutton 2019), by imposing structure on “the way to learn to solve a problem” rather than on the solutions or problems themselves.

As a generative classifier, the put of a manipulator enjoys some advantages over VAEs. But we found in Section 3.3 that the additional structure in the objective functions does not translate into increased task-specific performance. We suggested that this is because the put of manipulators approximate the Bayesian inversion of the get, and as a consequence, the put cannot be used to bootstrap the performance of a classifier, even when their inductive biases differ. Moreover, in Section 3.4 we found that, similarly to VAEs, training learners according to objective functions obtained from manipulation alone is insufficient in more complex domains, reflecting a more general drawback that price of an abstract vantage point is an inability to leverage domain-specific inductive biases and interventions. Whether these observations are invariant at scale, across modalities, and between tasks remains to be seen.

A broader goal for the pattern language is to map out a wider variety of machine learning models, relating them with refinement relations as already hinted at in this work. Furthermore, we want to extend the language to incorporate other aspects of the objective function, for example, relating to work that focuses on the choice of model architecture (Khatri et al. 2024) and the underlying data distribution (Bronstein et al. 2021).

There is a creative art to deep learning that is done an injustice by attempts to systematise and derive-from-first-principles. Our priorities are accessibility, and the preference for expressive possibility over formal rigidity, and it is for these reasons that we pursue a diagrammatic pattern language for machine learning as a mode of communication and reasoning with minimal constraints.

## Acknowledgements

We would like to thank Steve Clark and Dimitri Kartsaklis for their helpful reviews. We are grateful to Nikhil Khatri, Jonathon Liu, Bob Coecke and the rest of the Quantinuum, Oxford office for all the insightful discussions. BR thanks Simon Harrison for his generous support via the Wolfson Harrison UK Research Council Quantum Foundation Scholarship.

## References

- Abou-Saleh, Faris, James Cheney, Jeremy Gibbons, James McKinna, and Perdita Stevens (2018). “Introduction to Bidirectional Transformations”. In: *Bidirectional Transformations: International Summer School, Oxford, UK, July 25-29, 2016, Tutorial Lectures*. Ed. by Jeremy Gibbons and Perdita Stevens. Cham: Springer International Publishing, pp. 1–28. ISBN: 978-3-319-79108-1. DOI: 10.1007/978-3-319-79108-1\_1. URL: [https://doi.org/10.1007/978-3-319-79108-1\\_1](https://doi.org/10.1007/978-3-319-79108-1_1).
- Alexander, Christopher, Sara Ishikawa, and Murray Silverstein (1977). *A Pattern Language: Towns, buildings, construction*. Vol. 2. Center for Environmental Structure Series. New York: Oxford University Press.
- Babaeizadeh, Mohammad, Chelsea Finn, Dumitru Erhan, Roy H. Campbell, and Sergey Levine (Mar. 2018). *Stochastic Variational Video Prediction*. arXiv: 1710.11252 [cs]. URL: <https://doi.org/10.48550/arXiv.1710.11252> (visited on 05/18/2024).
- Baez, John C. and Jade Master (Mar. 2020). “Open Petri Nets”. In: *Mathematical Structures in Computer Science* 30.3, pp. 314–341. ISSN: 0960-1295, 1469-8072. DOI: 10.1017/S0960129520000043. URL: <http://arxiv.org/abs/1808.05415> (visited on 03/17/2023).
- Bancilhon, Francois and Nicolas Spyratos (Dec. 1981). “Update semantics of relational views”. In: *ACM Trans. Database Syst.* 6.4, pp. 557–575. ISSN: 0362-5915. DOI: 10.1145/319628.319634. URL: <https://doi.org/10.1145/319628.319634>.

- Beck, Kent and Ward Cunningham (Sept. 1987). *Using Pattern Languages for Object-Oriented Programs*. Technical Report CR-87-43.
- Bengio, Samy, Oriol Vinyals, Navdeep Jaitly, and Noam Shazeer (2015). “Scheduled Sampling for Sequence Prediction with Recurrent Neural Networks”. In: *Advances in Neural Information Processing Systems*. Ed. by C. Cortes, N. Lawrence, D. Lee, M. Sugiyama, and R. Garnett. Vol. 28. Curran Associates, Inc. URL: [https://proceedings.neurips.cc/paper\\_files/paper/2015/file/e995f98d56967d946471af29d7bf99f1-Paper.pdf](https://proceedings.neurips.cc/paper_files/paper/2015/file/e995f98d56967d946471af29d7bf99f1-Paper.pdf).
- Boisseau, Guillaume and Paweł Sobociński (Nov. 2022). “String Diagrammatic Electrical Circuit Theory”. In: *Electronic Proceedings in Theoretical Computer Science* 372, pp. 178–191. ISSN: 2075-2180. DOI: 10.4204/EPTCS.372.13. URL: <http://arxiv.org/abs/2106.07763> (visited on 03/17/2023).
- Bonchi, Filippo, Robin Piedeleu, Paweł Sobociński, and Fabio Zanasi (June 2019). “Graphical Affine Algebra”. In: *2019 34th Annual ACM/IEEE Symposium on Logic in Computer Science (LICS)*, pp. 1–12. DOI: 10.1109/LICS.2019.8785877. URL: <https://doi.org/10.1109/LICS.2019.8785877>.
- Bonchi, Filippo, Paweł Sobociński, and Fabio Zanasi (Jan. 2017). “Interacting Hopf Algebras”. In: *Journal of Pure and Applied Algebra* 221.1, pp. 144–184. ISSN: 00224049. DOI: 10.1016/j.jpaa.2016.06.002. URL: <http://arxiv.org/abs/1403.7048> (visited on 05/17/2023).
- Bonchi, Filippo, Paweł Sobociński, and Fabio Zanasi (Sept. 2014). “A Categorical Semantics of Signal Flow Graphs”. In: *CONCUR 2014 - Concurrency Theory - 25th International Conference*. Rome, Italy. URL: <https://hal.science/hal-02134182>.
- Bond-Taylor, Sam, Adam Leach, Yang Long, and Chris G. Willcocks (Nov. 2022). “Deep Generative Modelling: A Comparative Review of VAEs, GANs, Normalizing Flows, Energy-Based and Autoregressive Models”. In: *IEEE Transactions on Pattern Analysis and Machine Intelligence* 44.11, pp. 7327–7347. ISSN: 0162-8828, 2160-9292, 1939-3539. DOI: 10.1109/TPAMI.2021.3116668. arXiv: 2103.04922 [cs, stat]. URL: <https://doi.org/10.48550/arXiv.2103.04922> (visited on 05/18/2024).
- Bowman, Samuel R., Luke Vilnis, Oriol Vinyals, Andrew Dai, Rafal Jozefowicz, and Samy Bengio (2016). “Generating Sentences from a Continuous Space”. In: *Proceedings of The 20th SIGNLL Conference on Computational Natural Language Learning*. Berlin, Germany: Association for Computational Linguistics, pp. 10–21. DOI: 10.18653/v1/K16-1002. URL: <https://doi.org/10.48550/arXiv.1511.06349> (visited on 05/18/2024).
- Bronstein, Michael M., Joan Bruna, Taco Cohen, and Petar Veličković (May 2021). *Geometric Deep Learning: Grids, Groups, Graphs, Geodesics, and Gauges*. DOI: 10.48550/arXiv.2104.13478. arXiv: 2104.13478 [cs, stat]. URL: <https://doi.org/10.48550/arXiv.2104.13478> (visited on 05/18/2024).
- Cho, Kenta and Bart Jacobs (Aug. 2019). “Disintegration and Bayesian Inversion via String Diagrams”. In: *Mathematical Structures in Computer Science* 29.7, pp. 938–971. ISSN: 0960-1295, 1469-8072. DOI: 10.1017/S0960129518000488. arXiv: 1709.00322 [cs]. URL: <https://doi.org/10.48550/arXiv.1709.00322> (visited on 05/18/2024).
- Chu, Casey, Andrey Zhmoginov, and Mark Sandler (2017). “Cyclegan, a master of steganography”. In: *arXiv preprint arXiv:1712.02950*. URL: <https://doi.org/10.48550/arXiv.1712.02950>.
- Ciampiconi, Lorenzo, Adam Elwood, Marco Leonardi, Ashraf Mohamed, and Alessandro Rozza (Jan. 2023). *A Survey and Taxonomy of Loss Functions in Machine Learning*. arXiv: 2301.05579 [cs]. URL: <https://doi.org/10.48550/arXiv.2301.05579> (visited on 05/18/2024).
- Coecke, Bob and Ross Duncan (Apr. 2011). “Interacting quantum observables: categorical algebra and diagrammatics”. In: *New Journal of Physics* 13.4, p. 043016. DOI: 10.1088/1367-2630/13/4/043016. URL: <https://dx.doi.org/10.1088/1367-2630/13/4/043016>.
- Coecke, Bob and Aleks Kissinger (2017). *Picturing Quantum Processes: A First Course in Quantum Theory and Diagrammatic Reasoning*. Cambridge: Cambridge University Press. ISBN: 978-1-107-10422-8. DOI: 10.1017/97811316219317. URL: <https://www.cambridge.org/core/books/picturing-quantum-processes/1119568B3101F3A685BE832FEEC53E52> (visited on 03/17/2023).

- Coecke, Bob, Mehrnoosh Sadrzadeh, and Stephen Clark (Mar. 2010). *Mathematical Foundations for a Compositional Distributional Model of Meaning*. DOI: 10.48550/arXiv.1003.4394. URL: <http://arxiv.org/abs/1003.4394> (visited on 05/18/2023).
- Cruttwell, Geoffrey SH, Bruno Gavranović, Neil Ghani, Paul Wilson, and Fabio Zanasi (2022). “Categorical foundations of gradient-based learning”. In: *Programming Languages and Systems: 31st European Symposium on Programming, ESOP 2022, Held as Part of the European Joint Conferences on Theory and Practice of Software, ETAPS 2022, Munich, Germany, April 2–7, 2022, Proceedings*. Springer International Publishing Cham, pp. 1–28. URL: <https://doi.org/10.48550/arXiv.2103.01931>.
- Dziugaite, Gintare Karolina, Zoubin Ghahramani, and Daniel M. Roy (Aug. 2016). *A Study of the Effect of JPG Compression on Adversarial Images*. arXiv: 1608.00853 [cs]. URL: <https://doi.org/10.48550/arXiv.1608.00853> (visited on 05/18/2024).
- Fong, Brendan and David I. Spivak (Aug. 2019). *Supplying Bells and Whistles in Symmetric Monoidal Categories*. URL: <https://doi.org/10.48550/arXiv.1908.02633> (visited on 03/24/2024).
- Fox, Thomas (Jan. 1976). “Coalgebras and Cartesian Categories”. In: *Communications in Algebra* 4.7, pp. 665–667. ISSN: 0092-7872, 1532-4125. DOI: 10.1080/0092787608822127. URL: <https://doi.org/10.1080/0092787608822127> (visited on 03/05/2024).
- Fritz, Tobias (Aug. 2020). “A Synthetic Approach to Markov Kernels, Conditional Independence and Theorems on Sufficient Statistics”. In: *Advances in Mathematics* 370, p. 107239. ISSN: 00018708. DOI: 10.1016/j.aim.2020.107239. arXiv: 1908.07021 [cs, math, stat]. URL: <https://doi.org/10.1016/j.aim.2020.107239> (visited on 05/18/2024).
- Fritz, Tobias, Tomáš Gonda, and Paolo Perrone (Nov. 2021). “De Finetti’s Theorem in Categorical Probability”. In: *Journal of Stochastic Analysis* 2.4. ISSN: 2689-6931. DOI: 10.31390/josa.2.4.06. URL: <http://arxiv.org/abs/2105.02639> (visited on 03/17/2023).
- Fu, Huan, Mingming Gong, Chaohui Wang, Kayhan Batmanghelich, Kun Zhang, and Dacheng Tao (June 2019). “Geometry-Consistent Generative Adversarial Networks for One-Sided Unsupervised Domain Mapping”. In: *Proceedings of the IEEE/CVF Conference on Computer Vision and Pattern Recognition (CVPR)*.
- Goodfellow, Ian, Jean Pouget-Abadie, Mehdi Mirza, Bing Xu, David Warde-Farley, Sherjil Ozair, Aaron Courville, and Yoshua Bengio (2020). “Generative adversarial networks”. In: *Communications of the ACM* 63.11, pp. 139–144. URL: <https://doi.org/10.1145/3422622>.
- Haydon, Nathan and Paweł Sobociński (2020). “Compositional Diagrammatic First-Order Logic”. en. In: *Diagrammatic Representation and Inference*. Ed. by Ahti-Veikko Pietarinen, Peter Chapman, Leonie Bosveld-de Smet, Valeria Giardino, James Corter, and Sven Linker. Lecture Notes in Computer Science. Cham: Springer International Publishing, pp. 402–418. ISBN: 978-3-030-54249-8. DOI: 10.1007/978-3-030-54249-8\_32. URL: [https://doi.org/10.1007/978-3-030-54249-8\\_32](https://doi.org/10.1007/978-3-030-54249-8_32).
- Hedges, Jules (Mar. 2015). *String diagrams for game theory*. DOI: 10.48550/arXiv.1503.06072. URL: <http://arxiv.org/abs/1503.06072> (visited on 03/17/2023).
- Hertz, Amir, Ron Mokady, Jay Tenenbaum, Kfir Aberman, Yael Pritch, and Daniel Cohen-or (2022). “Prompt-to-Prompt Image Editing with Cross-Attention Control”. In: *The Eleventh International Conference on Learning Representations*. URL: <https://doi.org/10.48550/arXiv.2208.01626>.
- Hofmann, Martin, Benjamin Pierce, and Daniel Wagner (2011). “Symmetric lenses”. In: *ACM SIGPLAN Notices* 46.1, pp. 371–384.
- Hornik, Kurt, Maxwell Stinchcombe, and Halbert White (1989). “Multilayer feedforward networks are universal approximators”. In: *Neural networks* 2.5, pp. 359–366.
- Jacobs, Bart, Aleks Kissinger, and Fabio Zanasi (2019). “Causal inference by string diagram surgery”. In: *Foundations of Software Science and Computation Structures: 22nd International Conference, FOSSACS 2019, Held as Part of the European Joint Conferences on Theory and Practice of Software, ETAPS 2019, Prague, Czech Republic, April 6–11, 2019, Proceedings* 22. Springer, pp. 313–329. URL: [https://doi.org/10.1007/978-3-030-17127-8\\_18](https://doi.org/10.1007/978-3-030-17127-8_18).

- Kawar, Bahjat, Shiran Zada, Oran Lang, Omer Tov, Huiwen Chang, Tali Dekel, Inbar Mosseri, and Michal Irani (June 2023). “Imagic: Text-Based Real Image Editing With Diffusion Models”. In: *Proceedings of the IEEE/CVF Conference on Computer Vision and Pattern Recognition (CVPR)*, pp. 6007–6017.
- Khatri, Nikhil, Tuomas Laakkonen, Jonathon Liu, and Vincent Wang-Maścianica (2024). *On the Anatomy of Attention*.
- Kingma, Diederik P. and Max Welling (Dec. 2022). *Auto-Encoding Variational Bayes*. DOI: 10.48550/arXiv.1312.6114. arXiv: 1312.6114 [cs, stat]. URL: <https://doi.org/10.48550/arXiv.1312.6114> (visited on 05/18/2024).
- Li, Juncen, Robin Jia, He He, and Percy Liang (2018). “Delete, Retrieve, Generate: a Simple Approach to Sentiment and Style Transfer”. In: *Proceedings of the 2018 Conference of the North American Chapter of the Association for Computational Linguistics: Human Language Technologies, Volume 1 (Long Papers)*, pp. 1865–1874. URL: <https://doi.org/10.18653/v1/N18-1169>.
- Liu, Ziwei, Ping Luo, Xiaogang Wang, and Xiaoou Tang (Dec. 2015). “Deep Learning Face Attributes in the Wild”. In: *Proceedings of International Conference on Computer Vision (ICCV)*.
- Lorenz, Robin and Sean Tull (Apr. 2023). *Causal models in string diagrams*. URL: <https://doi.org/10.48550/arXiv.2304.07638>.
- Müller, Samuel G. and Frank Hutter (2021). *TrivialAugment: Tuning-free Yet State-of-the-Art Data Augmentation*. arXiv: 2103.10158 [cs.CV].
- Ng, Andrew and Michael Jordan (2001). “On Discriminative vs. Generative Classifiers: A Comparison of Logistic Regression and Naive Bayes”. In: *Advances in Neural Information Processing Systems*. Vol. 14. MIT Press. (Visited on 05/18/2024).
- nLab authors (June 2024). *Bayesian inversion*. <https://ncatlab.org/nlab/show/Bayesian+inversion>. Revision 9.
- Panangaden, Prakash (Dec. 1999). “The Category of Markov Kernels”. In: *Electr. Notes Theor. Comput. Sci.* 22, pp. 171–187. DOI: 10.1016/S1571-0661(05)80602-4. URL: [https://doi.org/10.1016/S1571-0661\(05\)80602-4](https://doi.org/10.1016/S1571-0661(05)80602-4).
- Pavlovic, Dusko (2013). “Monoidal computer I: Basic computability by string diagrams”. In: *Information and Computation* 226. Special Issue: Information Security as a Resource, pp. 94–116. ISSN: 0890-5401. DOI: <https://doi.org/10.1016/j.ic.2013.03.007>. URL: <https://www.sciencedirect.com/science/article/pii/S0890540113000254>.
- (Sept. 2023). *Programs as Diagrams: From Categorical Computability to Computable Categories*. 1st ed. 2023 edition. Springer. ISBN: 978-3-031-34826-6. URL: <https://doi.org/10.48550/arXiv.2208.03817>.
- Poór, Boldizsár, Quanlong Wang, Razin A. Shaikh, Lia Yeh, Richie Yeung, and Bob Coecke (Apr. 2023). *Completeness for arbitrary finite dimensions of ZXW-calculus, a unifying calculus*. DOI: 10.48550/arXiv.2302.12135. URL: <http://arxiv.org/abs/2302.12135> (visited on 06/25/2023).
- Radford, Alec and Karthik Narasimhan (2018). “Improving Language Understanding by Generative Pre-Training”. In: URL: <https://api.semanticscholar.org/CorpusID:49313245>.
- Ranzato, Marc'Aurelio, Y-Lan Boureau, Sumit Chopra, and Yann LeCun (21–24 Mar 2007). “A Unified Energy-Based Framework for Unsupervised Learning”. In: *Proceedings of the Eleventh International Conference on Artificial Intelligence and Statistics*. Ed. by Marina Meila and Xiaotong Shen. Vol. 2. Proceedings of Machine Learning Research. San Juan, Puerto Rico: PMLR, pp. 371–379. URL: <https://proceedings.mlr.press/v2/ranzato07a.html>.
- Richardson, Oliver E. (28–30 Mar 2022). “Loss as the Inconsistency of a Probabilistic Dependency Graph: Choose Your Model, Not Your Loss Function”. In: *Proceedings of The 25th International Conference on Artificial Intelligence and Statistics*. Ed. by Gustau Camps-Valls, Francisco J. R. Ruiz, and Isabel Valera. Vol. 151. Proceedings of Machine Learning Research. PMLR, pp. 2706–2735. URL: <https://proceedings.mlr.press/v151/richardson22b.html>.

- Selinger, Peter (2011). “A Survey of Graphical Languages for Monoidal Categories”. In: *New Structures for Physics*. Ed. by Bob Coecke. Berlin, Heidelberg: Springer Berlin Heidelberg, pp. 289–355. ISBN: 978-3-642-12821-9. DOI: 10.1007/978-3-642-12821-9\_4. URL: [https://doi.org/10.1007/978-3-642-12821-9\\_4](https://doi.org/10.1007/978-3-642-12821-9_4).
- Shaikh, Razin A., Sara Sabrina Zemljic, Sean Tull, and Stephen Clark (Mar. 2022). *The Conceptual VAE*. DOI: 10.48550/arXiv.2203.11216. arXiv: 2203.11216 [cs]. URL: <https://doi.org/10.48550/arXiv.2203.11216> (visited on 05/18/2024).
- Sobociński, Paweł (June 2015). *Graphical Linear Algebra*. en. URL: <https://graphicallinearalgebra.net/> (visited on 05/17/2023).
- Sudhakar, Akhilesh, Bhargav Upadhyay, and Arjun Maheswaran (2019). ““Transforming” Delete, Retrieve, Generate Approach for Controlled Text Style Transfer”. In: *Proceedings of the 2019 Conference on Empirical Methods in Natural Language Processing and the 9th International Joint Conference on Natural Language Processing (EMNLP-IJCNLP)*, pp. 3269–3279. URL: <https://doi.org/10.48550/arXiv.1908.09368>.
- Sutton, Richard (2019). *The Bitter Lesson*. (Visited on 01/20/2023).
- Terven, Juan, Diana M. Cordova-Esparza, Alfonso Ramirez-Pedraza, and Edgar A. Chavez-Urbiola (Sept. 2023). *Loss Functions and Metrics in Deep Learning*. arXiv: 2307.02694 [cs]. URL: <https://doi.org/10.48550/arXiv.2307.02694> (visited on 05/18/2024).
- Vapnik, Vladimir N. (Sept. 1998). *Statistical Learning Theory*. 1st edition. New York: Wiley-Interscience. ISBN: 978-0-471-03003-4.
- Wang-Mascianica, Vincent, Jonathon Liu, and Bob Coecke (Jan. 2023). *Distilling Text into Circuits*. en. URL: <http://arxiv.org/abs/2301.10595> (visited on 04/27/2023).
- Watters, Nicholas, Loic Matthey, Sebastian Borgeaud, Rishabh Kabra, and Alexander Lerchner (2019). *Spriteworld: A Flexible, Configurable Reinforcement Learning Environment*. URL: <https://github.com/deepmind/spriteworld/>.
- Williams, Ronald J. and David Zipser (1989). “A Learning Algorithm for Continually Running Fully Recurrent Neural Networks”. In: *Neural Computation* 1.2, pp. 270–280. DOI: 10.1162/neco.1989.1.2.270. URL: <https://doi.org/10.1162/neco.1989.1.2.270>.
- Wu, Sidi, Yizi Chen, Samuel Mermet, Lorenz Hurni, Konrad Schindler, Nicolas Gonthier, and Loic Landrieu (Mar. 2024). *StegoGAN: Leveraging Steganography for Non-Bijective Image-to-Image Translation*. URL: <https://doi.org/10.48550/arXiv.2403.20142>.
- Yau, Donald (Sept. 2008). *Higher Dimensional Algebras via Colored PROPs*. arXiv: 0809.2161 [math-ph]. URL: <https://doi.org/10.48550/arXiv.0809.2161> (visited on 08/06/2019).
- Zhu, Jun-Yan, Taesung Park, Phillip Isola, and Alexei A Efros (2017). *Unpaired Image-to-Image Translation using Cycle-Consistent Adversarial Networks*.

## A Formal semantics

The functional effect of the construction below is to extend the category of continuous maps between Euclidean spaces with global elements that behave as probability distributions instead of points. We presume familiarity with symmetric monoidal categories and their graphical calculi (Selinger 2011).

Let **CartSp** denote the coloured PROP (Yau 2008) of continuous maps between Euclidean spaces, where the tensor product is the cartesian product — i.e. **CartSp** is cartesian monoidal.

Let **BorelStoch** denote the Markov category (Cho and Jacobs 2019; Fritz 2020) of stochastic kernels (Panangaden 1999) between Borel-measurable spaces. Stochastic kernels in particular subsume the continuous maps between Euclidean spaces.

As a Markov category, in the terminology of (Fong and Spivak 2019), **BorelStoch** supplies cocommutative comonoids. By Fox’s theorem (Fox 1976) cartesian monoidal categories are precisely those isomorphic to their own categories of cocommutative comonoids. Hence there is a (semicartesian) functorial embedding of **CartSp** into **BorelStoch** sending  $\mathbb{R}^N$  to  $\mathbb{R}^N$  (equipped with the usual



Borel measure), and continuous maps to deterministic continuous maps. We declare our semantic category to be generated by the image of this embedding along with the probability distributions  $\mathcal{X} : \{\star\} \rightarrow \mathbb{R}^N$ , where  $\{\star\}$  is the singleton monoidal unit of **BorelStoch**.

## B Deferred proofs

In this section, we refer to tasks and their realisations interchangeably: so instead of “manipulators” realising the manipulation task, we speak just of a manipulator, disambiguating when necessary.

### B.1 Proof of Proposition 3.3

CycleGANs (Task 2.8) solve a similar task as the strong manipulator, translating between two distributions. In fact, the strong manipulator is a refinement of CycleGANs, giving us more guarantees by avoiding certain failure cases. We can use the pattern language to show this formally. However, in both cases, the tasks are not perfectible, as, by design, it is impossible for the generator and the discriminator to have a loss of zero at the same time. Therefore, we have to generalise the definition of *refinement* for *partially perfectible tasks*.

**Definition B.1** (Partially perfectible task). A *partially perfectible task*  $\{(f_i, g_i, \mathcal{X}_i, \mathbb{P}_i)\}_i$  with learnable functions  $\Sigma_l$  is a compound task with excluded learners  $E \subseteq \Sigma_l$  such that:

1. no two  $e \in E$  share atomic tasks, i.e.  $\forall e, e' \in E. \{(f_i, g_i, \mathcal{X}_i, \mathbb{P}_i) | e \in f_i \vee e \in g_i\} \cap \{(f_i, g_i, \mathcal{X}_i, \mathbb{P}_i) | e' \in f_i \vee e' \in g_i\} = \emptyset$  and
2. all tasks not involving learners from  $E$  are perfectible, i.e.  $\exists \pi \in \mathbb{P}. \forall x \in X. f_i(\pi, x) = g_i(\pi, x)$

Importantly, there does not need to exist a perfect solution for all tasks. As condition (1) explicitly forbids excluded learners to share tasks, we do not need to make restrictions on their composite behaviour. An example of a partially perfectible task is CycleGAN with excluded learners  $\text{dsc}_1, \text{dsc}_2$ . Assuming an appropriate data distribution (Wu et al. 2024), the autoencoding tasks, i.e. the reconstruction losses, are perfectible. However, the generator-discriminator tasks are not. GAN with excluded learner  $\text{dsc}$  is another example of a partially perfectible tasks. In this case no tasks are required to be perfectible, as all of them involve the discriminator.

When we have partially perfectible tasks, we have to define what we mean by an optimal solution.

**Definition B.2** (Optimal partially perfect solution). Let  $\Phi = \{(f_i, g_i, \mathcal{X}_i, \mathbb{P}_i)\}_i$  be a partially perfectible tasks with learners  $\Sigma$  and excluded learners  $E \subseteq \Sigma$ . Then an *optimal partially perfect solution* for the learners  $L = \Sigma \setminus E$  is, if it exists, a set of parameters  $\pi_L \in \mathbb{P}_L$  such that for all  $\alpha_L, \mathbf{D}_\phi$  they perfect the perfectible tasks:

$$\forall \{(f_i, g_i, \mathcal{X}_i, \mathbb{P}_i) \in \Phi | \forall e \in E. e \notin f_i \wedge e \notin g_i\}. \forall x \in \mathcal{X}_i. f_i(\pi_L, x) = g_i(\pi_L, x)$$

and for all  $l \in L$  and all tasks  $\Phi_l$  with  $\text{para}(l) \cap \mathbb{P}_i \neq \emptyset$ :

$$\alpha_l(\{ \mathbb{E}_{x \sim \mathcal{X}_i} (\mathbf{D}_\phi(\text{sys}_\phi((\pi_L \cup \mathbb{P}_E(\pi_L)), x), \text{spec}_\phi(\pi_L \cup \mathbb{P}_E(\pi_L)), x)) | \phi \in \Phi_l \})$$

is minimal over all possible parameter combinations, where

$$\mathbb{P}_E(\pi_L) = \bigcup_{e \in E} \inf_{\pi_e \in \mathbb{P}_e} (\alpha_e(\{ \mathbb{E}_{x \sim \mathcal{X}_i} (\mathbf{D}_\psi(\text{sys}_\psi((\pi_L \cup \pi_L), x), \text{spec}_\psi((\pi_L \cup \pi_L), x)) | \psi \in \Phi_e \}))$$

In words, we consider a set of parameters *optimal partially perfect*, if they are perfect for the perfectible tasks and have a minimal objective function for the non-perfectible tasks, even if the

excluded learners only optimise for themselves. This may not always exist, either because there is no solution that is optimal for all  $\alpha_L, \mathbf{D}_\phi$  or as there may be more optimal solutions for the non-perfectible tasks that do not satisfy the perfectible tasks.

Given this, we can generalise the definition of *refinement* for partially perfectible tasks.

**Definition B.3** (Optimal refinement of partially-perfectible tasks). Given two partially-perfectible tasks  $\Psi, \Phi$  with excluded learners  $E_\Psi, E_\Phi$ , we say that  $\Psi$  optimally refines  $\Phi$  if optimal partially perfect solutions for  $\Sigma_{l_\Psi} \setminus E_\Psi$  can be composed to form optimal partially perfect solutions for  $\Sigma_{l_\Phi} \setminus A_\Phi$ .

For  $A_\Psi, A_\Phi = \emptyset$ , optimal refinement is equivalent to refinement.

To show that manipulation optimally refines cycleGAN, we need one assumption: we assume that the measure of statistical divergence and compound function have been chosen such that a generator in a generative-adversarial setting is optimal if and only if its output distribution is equal to the original distribution. As the goal of such a generative setting is to approximate the original distribution, this is quite a natural assumption. One possible choice of measure of statistical divergence and compound function is given by Goodfellow et al. (Goodfellow et al. 2020, Theorem 1) and has been proven to fulfil this assumption.

**Proposition B.4.** Given appropriately chosen measure of statistical divergence and compound functions, the strong manipulator with excluded learner dsc optimally refines the CycleGAN with excluded learners  $dsc_1, dsc_2$ .

*Proof.* Let  $\mathcal{X}_1, \mathcal{X}_2$  be two distributions over the same type. We create  $\mathcal{X} = (x, i)$  for  $x \in \mathcal{X}_i$  where the label  $i$  indicates the distribution the data point came from. Assuming that we have a strong manipulator (get, put, disc) with an optimal partially perfect put, get, we can construct optimal partially perfect generators  $G_1$  and  $G_2$  for CycleGAN.

For  $i \in 0, 1, j = 1 - i$ , we define:

$$G_i := \text{put} \triangleleft$$

First, we show that the perfectible tasks are indeed perfected, i.e. that both the autoencoder tasks are fulfilled. We have:

$$\begin{aligned} x_j \mid G_i G_j &= x_j \mid \text{put} \triangleleft \text{put} \triangleleft &= x_j \mid \text{put} \triangleleft & \text{(PutPut)} \\ & \text{(Def)} & & \\ &= x_j \mid \text{get} \text{put} &= x_j \mid & \text{(Classify)} \quad \text{(GetPut)} \end{aligned}$$

Next, we will show that these generators are indeed globally optimal. By assumption, a generator is optimal if and only if its output distribution is indistinguishable from the training distribution. Thus, assuming that the manipulator is optimal with respect to the generative-adversarial tasks, put output distribution approaches  $\mathcal{X} = (x, i)$  for  $x \in \mathcal{X}_i$ . But by PUTGET, we have:

$$x_j \mid G_i \text{get} = x_j \mid \text{put} \triangleleft \text{get} = x_j \mid \triangleleft \text{(PutGet)}$$

Therefore, by CLASSIFY,  $G_1$  and  $G_2$  can only return values that are akin to values in  $\mathcal{X}_1$  and  $\mathcal{X}_2$  respectively. As these two labels make up the entirety of  $\mathcal{X}$ ,  $G_1$ 's and  $G_2$ 's output distributions are indistinguishable from  $\mathcal{X}_1$  and  $\mathcal{X}_2$  respectively. Therefore, they are indeed optimal generators for their respective distribution.

But then we have shown that  $G_1$  and  $G_2$  are indeed optimal solutions to the CycleGAN pattern and therefore that the concept manipulator is a specialisation of the CycleGAN<sup>5</sup>.  $\square$

In turn, the CycleGAN, however, is not a refinement of the strong manipulator. This means there exist solutions to CycleGAN, which violate strong manipulator. In these image translation tasks, we expect the translators to change as little as possible to go from one distribution to the other, i.e. preserving as much information from the original as possible. However, the generators of the CycleGAN could, for example, flip the images horizontally. As the autoencoder tasks have an even number of generators on each side, this would be a ‘perfect solution’ to the outlined task, yet not the behaviour we would want or expect. In contrast, the PUTPUT rule of the strong manipulator does not allow this behaviour. As such, the strong manipulator gives us more guarantees than the CycleGAN.

Despite the additional guarantees, the strong manipulator does not guarantee that it indeed only changes as little as necessary to go from one distribution to the other. This can be seen when considering a limited toy scenario: the data has the four objects *circle*, *square*, *red* and *green*. There is no unique mapping between shapes and colours. Without further information, it is therefore completely impossible to say what it would mean to change as little as possible to go from shapes to colours. When considering this toy scenario, it becomes obvious that, without specifying further restrictions on all remaining attributes, it is impossible to know which mapping is correct. Yet, despite these theoretical concerns, in practice, even the weaker manipulator often converges to the desired behaviour, similar to CycleGANs, which have even fewer guarantees.

## B.2 Proof of Proposition 3.5

**Definition B.5** (Balanced entropy of an attribute). Given a distribution of data  $\mathcal{D}$  on space  $D$ , we say that a distribution  $\mathcal{A}$  over space  $A$  represents an *entropy-balanced attribute* of  $\mathcal{D}$  if there exists a complement type  $C$  with distribution  $\mathcal{C}$  such that we have the equality in distributions  $\mathcal{D} = \mathcal{A} \times \mathcal{C}$  up an isomorphism of the underlying spaces  $D \simeq (A \times C)$ .

**Task B.6** (entropy balancer). This task is autoencoder with a regularisation condition on the encoder to be satisfied in distribution.



**Lemma B.7** (Perfect-task representation of equal entropy). Balanced entropy in the attributes is equivalent to the perfectability of entropy balancer.

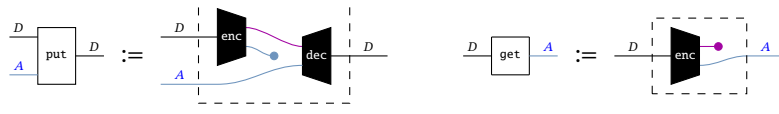
*Proof.* If there is balanced entropy in the attributes, Task B.6 may be satisfied up to identity by the enc and dec witnessing the isomorphism  $D \simeq (A \times C)$  that realises  $\mathcal{D} = \mathcal{A} \times \mathcal{C}$ . Conversely, if the task above are equalities, we recover the definition of balanced entropy.  $\square$

Contextually, we will assume that distributions have full support over spaces; this can always morally be the case by restrictions to subspaces. This assumption strengthens Lemma B.7 to yield the following corollary.

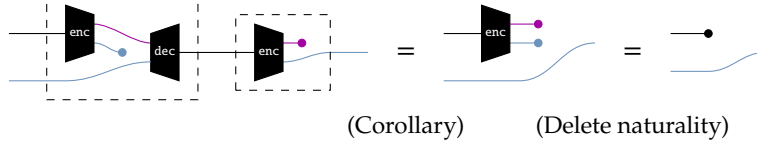
**Corollary B.8.** If entropy balancer is perfect, enc and dec witness an isomorphism  $D \simeq (A \times C)$ .

<sup>5</sup>In (Zhu et al. 2017), when doing style transfer, they additionally add the *identity loss* which enforces that generating an image in  $X_i$  given an image from  $X_1$  should return the identity. This perfectible task is also guaranteed by the strong manipulator by cIs and GetPut

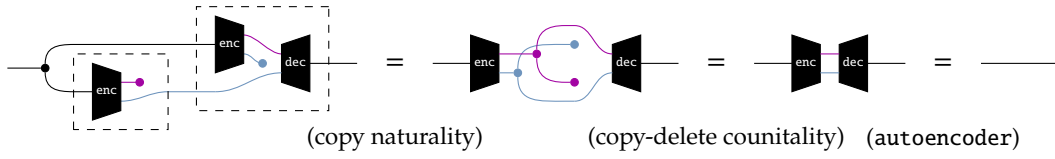
**Lemma B.9** (Hardcoding latent-spaces). Given a perfected entropy balancer, we may construct the following composites, which are the put and get of a strong manipulator<sup>6</sup>.



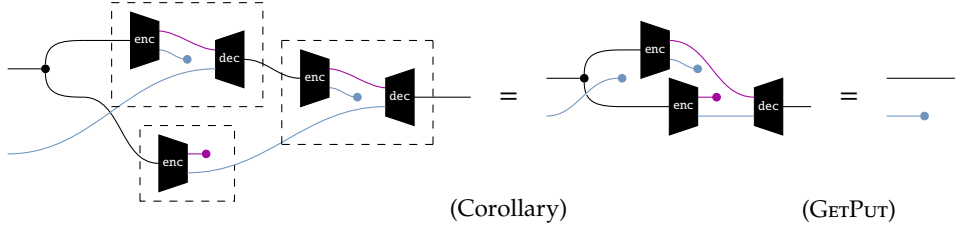
*Proof.* First, we argue that the lens laws are satisfied. PUTGET, GETPUT, UNDOABILITY, and PUTPUT follow from pure diagrammatic reasoning and applying Corollary B.8. For PUTGET:



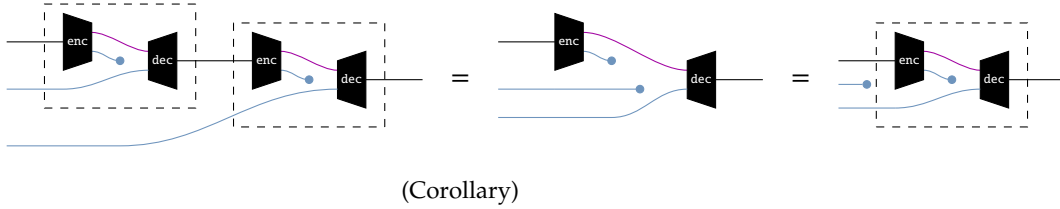
GETPUT:



UNDOABILITY:

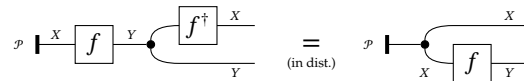


PUTPUT:



By construction, putting  $a$  by independently sampling the marginal on  $A$  is indistinguishable in distribution from the original distribution, hence the GAN laws of strong manipulator are optimally satisfied, and we are done.  $\square$

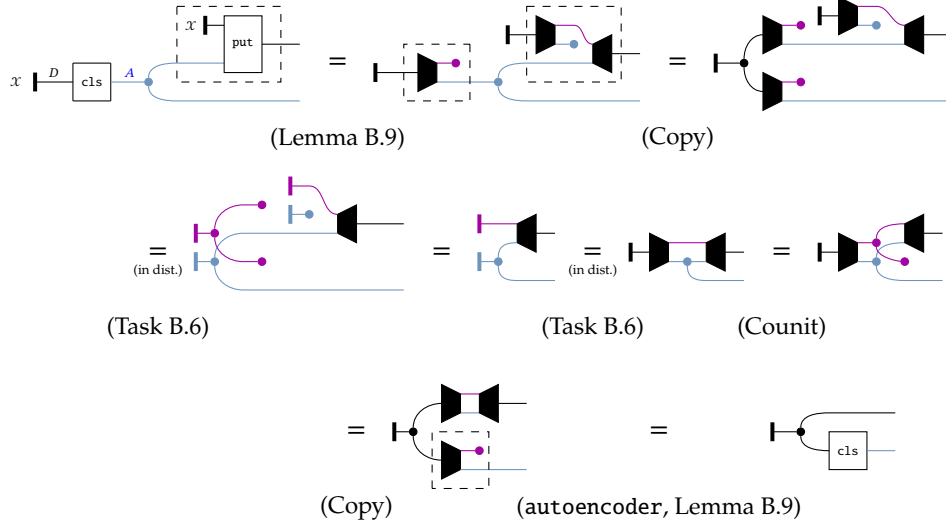
**Definition B.10** (Bayesian Inversion in Markov Categories). In a Markov category, the Bayesian inversion (Cho and Jacobs 2019; nLab authors 2024) of a stochastic map  $f : X \rightarrow Y$  with respect to a distribution  $\mathcal{P}$  on  $X$  is a stochastic map  $f^\dagger : Y \rightarrow X$  such that, in distribution:



<sup>6</sup>modulo CLASSIFY, which in this setting is trivially obtained as we assume the attribute is derived from get.

**Proposition B.11** (strong manipulator as Bayesian inversion). If a discriminative classifier  $\text{cls} : D \rightarrow A$  induces a balanced attribute  $\text{cls}(D)$  over  $A$  with respect to  $D$ , there exists a strong manipulator for which the put induces the Bayesian inversion  $\text{cls}^\dagger : A \rightarrow D$ .

*Proof.* We show that, under our premises, the put composed with an independent copy of the data source  $\mathcal{X}$  is the Bayesian inversion of  $\text{cls}$ .



□

## C Experiment Details

### C.1 Spriteworld

For the Spriteworld experiment, we procedurally generate 32x32 images containing a single shape with the following attributes:

<i>Attributes</i>	<i>Possible Values</i>
Shape	{ Ellipse, Rectangle, Triangle }
Hue	{ Red : $0 \pm 8$ , Green : $85 \pm 8$ , Blue : $170 \pm 8$ }
Saturation	64-255
Value	64-255
Background Color	Black
Width & Height	5-27
X & Y position	5-27

Only the first two attributes, shape and hue, are changed in the manipulation task, but all unchanged properties are intended to be preserved by the transformation. We use an autoencoder with a CNN/DCNN architecture to embed each image into a latent space:

<i>Parameter</i>	<i>Value</i>
Latent Size	32
Layers	4
Hidden Channels	64
Kernel Size	5x5
Stride	2
Activation Function	LeakyReLU(0.1) followed by BatchNorm

We train separate *get*/*put* models for each of the three concepts: shape, colour, blue-circleness. Each model uses the encoder of the autoencoder to embed input images into latent space, and only sees the labels for the particular attribute it is manipulating.

For shape and colour, the *get* model uses a linear classifier from the latent space (of size 32) to 3 output logit values, one for each possible value. The *put* model maps a one-hot vector of the input value to a vector in latent space that is added to the embedding. This new embedding is then decoded by the autoencoder.

For blue-circleness, the *get* model uses a linear classifier from the latent space to a single output value from zero to one (we do not use a sigmoid output layer to restrict the output). The *put* model uses a complement of size 8. It concatenates the one-hot value vector with the image embedding and the complement vector (using a default trainable complement vector if one is not provided) and passes that through a linear layer to get a new embedding vector (which is then decoded) and complement vector.

In total, these models contain 644,130 parameters. All models are trained simultaneously according to the autoencoding and manipulation rules, along with *PUTPUT*. At each step, a batch of images is generated, along with four batches of random values, containing random labels for the shape and colour manipulators, and random real numbers for the blue-circleness manipulator, uniformly sampled from  $[-0.1, 1.1]$  and then clamped to  $[0, 1]$ . The loss function is a weighted sum of the losses from each atomic task in order to balance the signal from the image loss with the signal from the classifier loss:

<i>Hyper-parameter</i>	<i>Value</i>	<i>Task</i>	<i>Weight</i>
Steps	100,000	AUTOENCODING	100
Batch Size	512	GETPUT	1
Optimiser	AdamW	PUTPUT	1
Learning Rate	$10^{-3}$	UNDO	10
Weight Decay	$10^{-2}$	PUTGET	
Gradient Clipping	1 (element-wise)	(blue-circleness)	10
Image Loss	$L_2 + 0.25 \cdot L_1$	(shape and colour)	1
Discrete Value Loss	Binary cross-entropy	CLASSIFICATION	
Continuous Value Loss	Mean squared error	(blue-circleness)	10
Seed	0	(shape and colour)	1

## C.2 Faces

For the faces experiment, we use the *CelebFaces Attributes* dataset (Z. Liu et al. 2015), with an off-the-shelf data augmentation method called “TrivialAugment” (Müller and Hutter 2021). Again, we use an autoencoder with a CNN/DCNN architecture to embed each image:

<i>Parameter</i>	<i>Value</i>
Latent Size	128
Layers	5
Hidden Channels	8, 16, 32, 64, 128
Kernel Size	5
Stride	2
Activation Function	LeakyReLU(0.1) followed by BatchNorm

We train linear `get/put` models for the binary concept of “Smiling”, resulting in a total of 1,071,749 parameters. The loss function is a weighted sum of the losses from each atomic task:

<i>Hyper-parameter</i>	<i>Value</i>	<i>Task</i>	<i>Weight</i>
Steps	100,000	AUTOENCODING	10
Batch Size	64	GETPUT	1
Optimiser	AdamW	PUTPUT	1
Learning Rate	$10^{-3}$	UNDO	1
Weight Decay	$10^{-2}$	PUTGET	1
Gradient Clipping	1 (element-wise)	CLASSIFICATION	1
Image Loss	$L_2 + 0.2 \cdot L_1 + SSIM$		
Value Loss	Binary cross-entropy		
Seed	0		

### C.3 MNIST

We trained the `manipulator` pattern on the MNIST dataset, using the digit label as the property. The `get` operated directly on images, while `put` was trained to act on the latent space of an autoencoder, as in option (1) of Section 3.2. The images are input as  $28 \times 28$  matrices, flattened to 784-dimensional vectors, and the labels are provided as 10-dimensional vectors with one-hot encoding. All of the components were structured as multilayer perceptrons. The hyperparameters are given below:

	<code>enc</code>	<code>dec</code>	<code>put</code>	<code>get</code>
Input Dimension	$784 = 28 \times 28$	32	$42 = 32 + 10$	$784 = 28 \times 28$
Output Dimension	32	$784 = 28 \times 28$	32	10
Hidden Dimensions	{128, 128, 64}	{64, 128, 128}	{128, 128, 128}	{64, 64}
Hidden Activations	ReLU	ReLU	ReLU	ReLU
Final Activation	Sigmoid	Sigmoid	Sigmoid	Softmax

With these components, we performed four tasks: (a) training `get` supervised, (b) training `get` given pre-trained `put`, `enc`, and `dec`, (c) training `put` given pre-trained `get`, `enc`, and `dec`, and (d) training `get` to match a previous `get`. These were trained using the `manipulation` rules, as well as `PUTPUT`, and additional regularization term we denote as `ENTROPY`. The loss function of `ENTROPY` is given by

$$\mathcal{L}_{\text{ENTROPY}} = \mathbb{E}[H(\text{get}(\text{enc}(x)))] - H(\mathbb{E}[\text{get}(\text{enc}(x))])$$

where  $x$  is a batch of input images,  $H(\cdot)$  is the entropy of a categorical distribution, and the expectation is approximated by the mean over each batch. The idea behind `ENTROPY` is to encourage the output of `get` to be well-distributed across labels (by maximizing the entropy of the mean distribution) but to be sure of each label (by minimizing the entropy for each specific input). For task (d), labels were generated for the `CLASSIFY` rule using `get`. Each task is trained by minimizing a weighted linear

combination of the rules. We give the hyperparameters, rule weights, and loss functions for each of these below.

	(a)		(b)		(c)		(d)	
Optimizer	Adam		Adam		Adam		Adam	
Learning Rate	0.001		0.001		0.0001		0.001	
Epochs	20		20		20		20	
	<i>Weight</i>	<i>Loss</i>	<i>Weight</i>	<i>Loss</i>	<i>Weight</i>	<i>Loss</i>	<i>Weight</i>	<i>Loss</i>
CLASSIFY	1	CE	–	–	–	–	1	CE
PUTGET	–	–	10	CE	10	CE	–	–
GETPUT	–	–	10	L2	10	L2	–	–
PUTPUT	–	–	10	L2	10	L2	–	–
UNDOABILITY	–	–	10	L2	10	L2	–	–
ENTROPY	–	–	1	$\mathcal{L}_{\text{ENTROPY}}$	–	–	–	–

We also have an additional task (e) of training enc and dec unsupervised. This was done using the Adam optimizer, with a learning rate of 0.001 for 80 epochs. The reconstruction loss was given by

$$\mathcal{L}(x, \hat{x}) = \text{L2}(x, \hat{x}) + (1 - \text{SSIM}(x, \hat{x}))$$

where SSIM is the structure similarity image metric. Finally, we have the tasks (f) training a VAE to learn the joint distribution of images and labels produced by get', and (g) training a get supervised using labels and images generated from the VAE. The VAE encoder and decoder are also based on multilayer perceptrons - each is comprised of an MLP trunk and two linear heads for generating the means and log-variances of the latent space, or the image and labels, respectively. The latent space is comprised of independent normally distributed variables as in (Kingma and Welling 2022), and is sampled using the standard reparameterization trick. The hyperparameters of the architecture are given below:

	VAE Encoder	VAE Decoder
Input Dimension	794 = 28 × 28 + 10	32
Hidden Dimensions	{128, 128, 64}	{64, 128, 128}
Hidden Activations	ReLU	ReLU
Head 1 Dimension	32	784 = 28 × 28
Head 1 Activation	–	Sigmoid
Head 2 Dimension	32	10
Head 2 Activation	–	Softmax

Three loss functions were used for tasks (f) and (g) — the reconstruction loss of the autoencoder, which can be separated into a label loss and an image loss, the K-L divergence regularization term  $\mathcal{L}_{KL}$  of the VAE (Kingma and Welling 2022), and the CLASSIFY loss of get. The training hyperparameters are given as follows:



	(f)		(g)	
Optimizer	Adam		Adam	
Learning Rate	0.001		0.001	
Epochs	40		20	
	<i>Weight</i>	<i>Loss</i>	<i>Weight</i>	<i>Loss</i>
CLASSIFY	–	–	1	CE
Image Reconstruction	100	L2	–	–
Label Reconstruction	1	CE	–	–
K-L Divergence	0.5	$\mathcal{L}_{KL}$	–	–

In order to evaluate the three methods given in Section 3.3, we trained the tasks in the following order. At each step, the component being trained (e.g. `get`, `put`, etc) was initialized randomly (the previous weights were discarded). Measurements of the test accuracy were made after each (a), (b), (d), or (g) training run, and used to produce Figure 5(b).

$$\begin{aligned} \text{get} \rightarrow \text{get}' &\implies (a) \rightarrow (d) \rightarrow (d) \rightarrow \dots \rightarrow (d) \\ \text{get} \rightarrow \text{put} \rightarrow \text{get}' &\implies (a) \rightarrow (e) \rightarrow (c) \rightarrow (b) \rightarrow (e) \rightarrow (c) \rightarrow (b) \rightarrow \dots \rightarrow (b) \\ \text{get} \rightarrow \text{VAE} \rightarrow \text{get}' &\implies (a) \rightarrow (f) \rightarrow (g) \rightarrow (f) \rightarrow (g) \rightarrow \dots \rightarrow (g) \end{aligned}$$

To produce Figure 5(a), an `enc`, `dec`, `put`, and `get` were trained using (a)  $\rightarrow$  (e)  $\rightarrow$  (c), followed by training (c) for an additional 40 epochs. A slightly larger (but still MLP-based) model, where both `put` and `get` act on the latent space of the autoencoder, was used to achieve better visual quality. The hyperparameters are detailed below:

	<code>enc</code>	<code>dec</code>	<code>put</code>	<code>get</code>
Input Dimension	784 = 28 × 28	32	42 = 32 + 10	32
Output Dimension	32	784 = 28 × 28	32	10
Hidden Dimensions	{128, 128, 128, 32, 32}	{32, 32, 128, 128, 128}	{256, 256}	{256}
Hidden Activations	ReLU	ReLU	ReLU	ReLU
Final Activation	Sigmoid	Sigmoid	Sigmoid	Softmax

`enc`, `dec`, and `put` were used to manipulate six examples picked from the dataset, putting each of the ten classes onto each example. The examples were cherry-picked to provide maximum stylistic contrast across the sample but were not selected for maximum style transfer accuracy - a similar level was observed across the entire dataset. Code for all of these models, as well as the training schedules of tasks (a)-(g), are provided in the supplementary material.

## C.4 Sentiment Manipulation

For the sentiment manipulation task, we pretrained the Blind Generative Style Transformer (**B-GST**) model of (Sudhakar, Upadhyay, and Maheswaran 2019) which takes in the non-stylistic components of a sentence and the target sentiment, and outputs the sentence generated in the target style. This was done until we achieved baselines higher than the original ones reported by the authors of the model. Afterwards, we continued training under three different conditions: (1) resuming training with only the original objective, (2) only using objective functions from manipulation, and (3) using both. For (1) and (3), we reused the same objective in the original paper. In all experiments, we used the YELP dataset used by (Li et al. 2018), reusing the same train-dev-test split they used. It consists of 270K positive and 180K negative sentences for the training set, 2000 sentences each for the

dev set, and 500 sentences each for the test set. Furthermore, we used the human gold standard references they provided for their test set. **B-GST** uses a sequence length of 512, 12 attention blocks each with 12 attention heads. We used 768-dimensional internal states (keys, queries, values, word embeddings, positional embeddings). We tokenized the input text using Byte-Pair Encoding (BPE).

We used the same input autoencoding and output decoding used in (Sudhakar, Upadhyay, and Maheswaran 2019) across all experiments. For the `get` of the manipulation task, we used the PyTorch version of the pretrained Transformer by HuggingFace, which uses the OpenAI GPT model pretrained by (Radford and Narasimhan 2018) on the BookCorpus dataset which contains over 7000 books with approximately 800M words. We trained it on a sentiment classification task using the YELP dataset reaching 98% accuracy on the test set. The `get` was fixed for the entire duration of training conditions (2) and (3) above. For the `put` of manipulation, we used the **B-GST** model to generate text with a specified sentiment. This was a computational bottleneck for training conditions (2) and (3) as autoregressive decoding is required to generate model inputs for `PUTGET` and `UNDOABILITY` in manipulation. We used 'teacher forcing' or 'guided approach' (Bengio et al. 2015; Williams and Zipser 1989) whenever we computed the reconstruction loss of `put`. Additionally, for training conditions (2) and (3), we only used `PUTGET`, `GETPUT`, and `UNDOABILITY` from manipulation. We used a weighted sum of the losses computed for each of these and the original reconstruction loss if present - the weights can be considered as training hyperparameters. For (2), we used (`PUTGET`=5, `GETPUT`=20, `UNDOABILITY`=20), while for (3), we used (`PUTGET`=5, `GETPUT`=10, `UNDOABILITY`=25, `B-GST`=30). Code for all of the models, training schedules, and hyperparameter values for training conditions (1)-(3) are also provided in the supplementary material.